Traffic 2011; **12:** 1119–1123

doi:10.1111/j.1600-0854.2011.01229.x

Traffic Interchange

A Conserved Archaeal Pathway for Tail-Anchored Membrane Protein Insertion

John Sherrill[1], Malaiyalam Mariappan[2], Pawel Dominik[1], Ramanujan S. Hegde[2,3] and Robert J. Keenan[1,*]

[1]Department of Biochemistry & Molecular Biology, University of Chicago, Gordon Center for Integrative Science, Room W238, Chicago, IL 60637, USA
[2]Cell Biology and Metabolism Program, National Institute of Child Health and Human Development, National Institutes of Health, Room 101, Building 18T, 18 Library Drive, Bethesda, MD 20892, USA
[3]Present address: MRC Laboratory of Molecular Biology, Hills Road, Cambridge, CB2 0QH, United Kingdom
**Corresponding author: Robert J. Keenan, bkeenan@uchicago.edu*

Eukaryotic tail-anchored (TA) membrane proteins are inserted into the endoplasmic reticulum by a post-translational TRC40 pathway, but no comparable pathway is known in other domains of life. The crystal structure of an archaebacterial TRC40 sequence homolog bound to ADP•AlF_4^- reveals characteristic features of eukaryotic TRC40, including a zinc-mediated dimer and a large hydrophobic groove. Moreover, archaeal TRC40 interacts with the transmembrane domain of TA substrates and directs their membrane insertion. Thus, the TRC40 pathway is more broadly conserved than previously recognized.

Key words: archaea, ArsA, Get3, insertion, post-translational targeting, tail-anchored membrane proteins, TRC40

Received 11 April 2011, revised and accepted for publication 8 June 2011, uncorrected manuscript published online 9 June 2011, published online 3 July 2011

Eukaryotic tail-anchored (TA) proteins are found in all intracellular membranes where they perform wide-ranging functions (1–4). Those destined for compartments of the secretory pathway are inserted into the endoplasmic reticulum (ER) membrane by a recently discovered post-translational targeting pathway (5–9). Newly synthesized TA proteins are first captured by the mammalian Bag6-TRC35-Ubl4A 'pretargeting' complex or its yeast ortholog, Sgt2-Get4-Get5 (10–13). Next, the TA substrate is transferred to a cytosolic ATPase, called transmembrane domain recognition complex (TRC) 40 (Get3 in yeast) (5,7), which targets to its ER-localized membrane receptor, WRB (Get1/2 in yeast) (8,14). Subsequently, the TA substrate is inserted into the membrane and TRC40/Get3 is recycled to the cytosol. The multiple components of this conserved eukaryotic targeting pathway ensure selectivity for the ER membrane and minimize TA protein aggregation in the cytosol (8,15,16).

Archaeal and bacterial genomes also encode TA proteins (17), but the mechanism underlying their insertion into the prokaryotic plasma membrane is not known. Indeed, given their simple membrane system, the relatively small number of predicted TA proteins (17) and the feasibility of 'unassisted' insertion (18), it is not known whether archaea or bacteria even require a specialized post-translational TA membrane protein targeting system.

The identification of archaeal sequence homologs of eukaryotic TRC40/Get3 led to the proposal that archaea possess a TA protein targeting pathway similar to that in eukaryotes (17). To test this, we first determined the X-ray crystal structure of ADP•AlF_4^--bound TRC40 from the methanogen *Methanothermobacter thermautotrophicus* at 2.1 Å resolution (Table S1, Figure S1 and *Methods*). The archaeal enzyme adopts the same 'closed' conformation observed in the ADP•AlF_4^--bound form of *Saccharomyces cerevisiae* Get3 (19) (Figure 1A,B) (~36% sequence identity; RMSD Cα of 0.78 Å over 194 residues). This closed conformation results in an extensive dimer interface that spans the ATPase- and α-helical subdomains and buries two active-site nucleotides in a head-to-head conformation at the interface. The two monomers are linked by a zinc ion that is co-ordinated by four cysteine residues. These cysteines, two from each monomer, are part of the conserved 'CXXC' motif found in all known eukaryotic TRC40/Get3 orthologs, but not in functionally unrelated bacterial ArsA sequence homologs (Figure 2).

The most striking structural feature of ADP•AlF_4^--bound archaeal TRC40 is a large hydrophobic groove located at the dimer interface (Figure 1A,C,D). A similar feature, observed in the ADP•AlF_4^--bound structure of yeast Get3 (Figure 1B,E), has been implicated as the site of transmembrane domain (TMD) binding by a combination of structural, biochemical and genetic analysis (19–23). In archaea, as in yeast, the composite groove is constructed from a series of flexible, amphipathic helices. Notably, helix α8 (part of the 'TRC40-insert' sequence motif), which is observed in 'open' conformations of yeast Get3 (19,21,23), is absent from the MtTRC40 structure. Instead, helices α7 and α9 form an extended hairpin structure connected by an ~12-residue loop (Figure 1A). In the crystal, the hydrophobic surface of this loop interacts with the corresponding loop from a symmetry-related molecule. As is true for eukaryotic TRC40/Get3 orthologs,

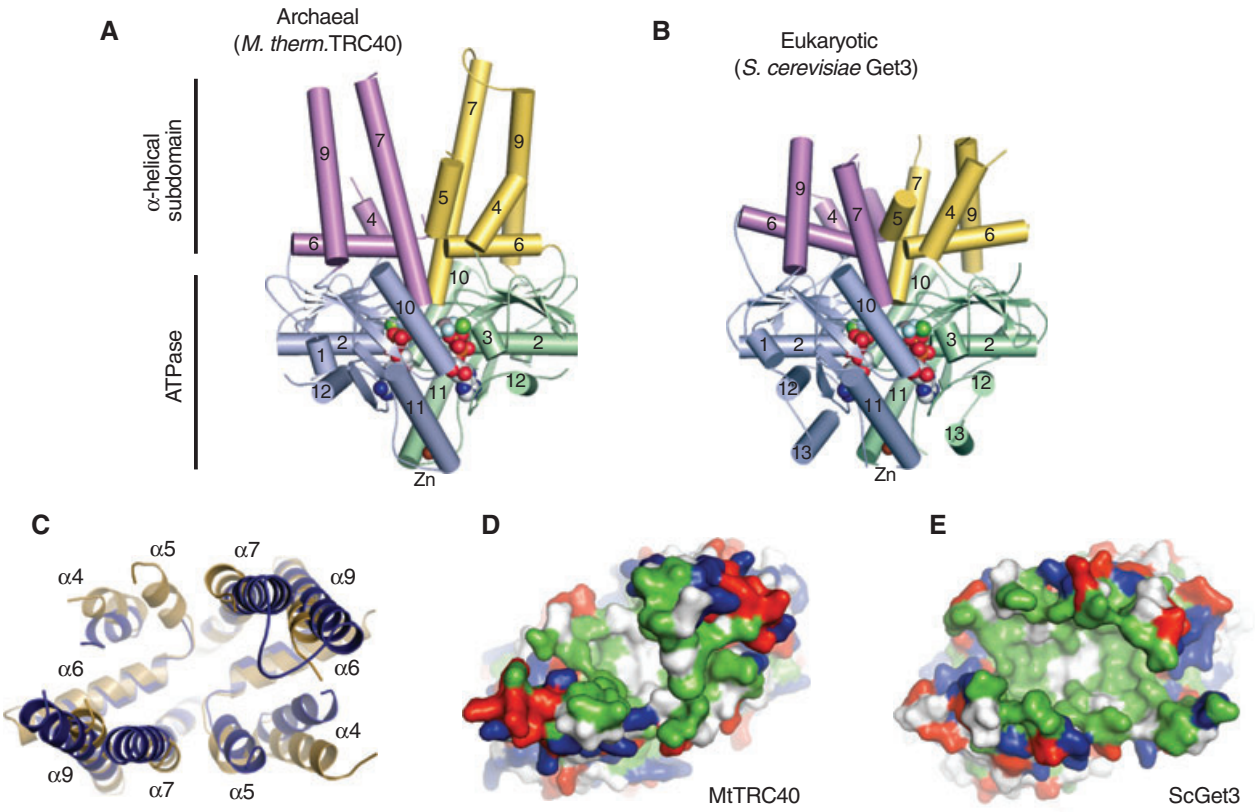

Figure 1: An evolutionarily conserved hydrophobic groove in archaeal TRC40. Comparison of (A) *M. thermautotrophicus* TRC40 and (B) *S. cerevisiae* Get3 $Mg^{2+}ADP{\bullet}AlF_4^-$ complexes (19). The ATPase domains are colored blue and green; α-helical subdomains are colored magenta and yellow; nucleotides and metals are shown as spheres. C) Overlay of the composite hydrophobic groove in MtTRC40 (dark blue) and ScGet3 (gold). Surface representations of the closed dimer grooves from (D) MtTRC40 and (E) ScGet3, oriented as in (C). Hydrophobic residues are colored green; positively and negatively charged residues are colored blue and red, respectively.

the non-polar and methionine-rich character of the groove is conserved across archaeal TRC40s (Figure 2) (17,19).

The conservation of key structural features suggested that the archaeal and eukaryotic TRC40 homologs share a common function. To address this directly, we asked whether MtTRC40 interacts with TA substrates *in vitro*. Cross-linking analysis in a rabbit reticulocyte lysate (RRL) translation extract supplemented with purified MtTRC40 revealed a strong interaction with full-length human Sec61β (a model TA protein) (Figure 3A). In contrast, an insertion-deficient 'triple arginine' Sec61β mutant and a construct lacking a TMD fail to interact appreciably with MtTRC40 (Figure 3A). Thus, as is observed with eukaryotic TRC40 (11), TMD hydrophobicity is an important determinant of TA protein binding to MtTRC40.

We also examined whether archaeal TRC40 could functionally replace the endogenous mammalian TRC40 at physiological concentrations. When added to an RRL translation extract depleted of TRC40 and pretargeting factors, MtTRC40 could be cross-linked efficiently to Sec61β (Figure 3B). This cross-link was lost upon incubation with yeast rough microsomes (yRMs) (prepared from a ΔGet3 strain) but not liposomes (Figure 3B), suggesting that the TA protein had inserted into the yRM membrane.

To test this, we used a protease-protection assay to measure insertion of these MtTRC40–Sec61β complexes. Strikingly, Sec61β inserted efficiently into yRMs, but not into the protein-free liposomes (Figure 3C). Moreover, microsomes from ΔGet1 or ΔGet2 yeast strains displayed reduced levels of insertion, while ΔGet3 microsomes were similar to wild-type yRMs (Figure 3C).

The discovery of a structurally and biochemically conserved TA protein targeting factor in archaea indicates that the post-translational TRC40 pathway is more broadly conserved than previously appreciated. The absence of recognizable sequence homologs for any of the upstream eukaryotic components (e.g. Sgt2, Bag6, TRC35 or Ubl4A) suggests that the archaeal pathway represents a simplified and ancient predecessor. That MtTRC40 directs insertion into yRMs in a Get1- and Get2-stimulated manner is consistent with a functionally orthologous integral membrane receptor in archaea. If this were the case, the primary sequence identity is apparently limited as no clear homolog to eukaryotic WRB, Get1 or Get2 is seen in

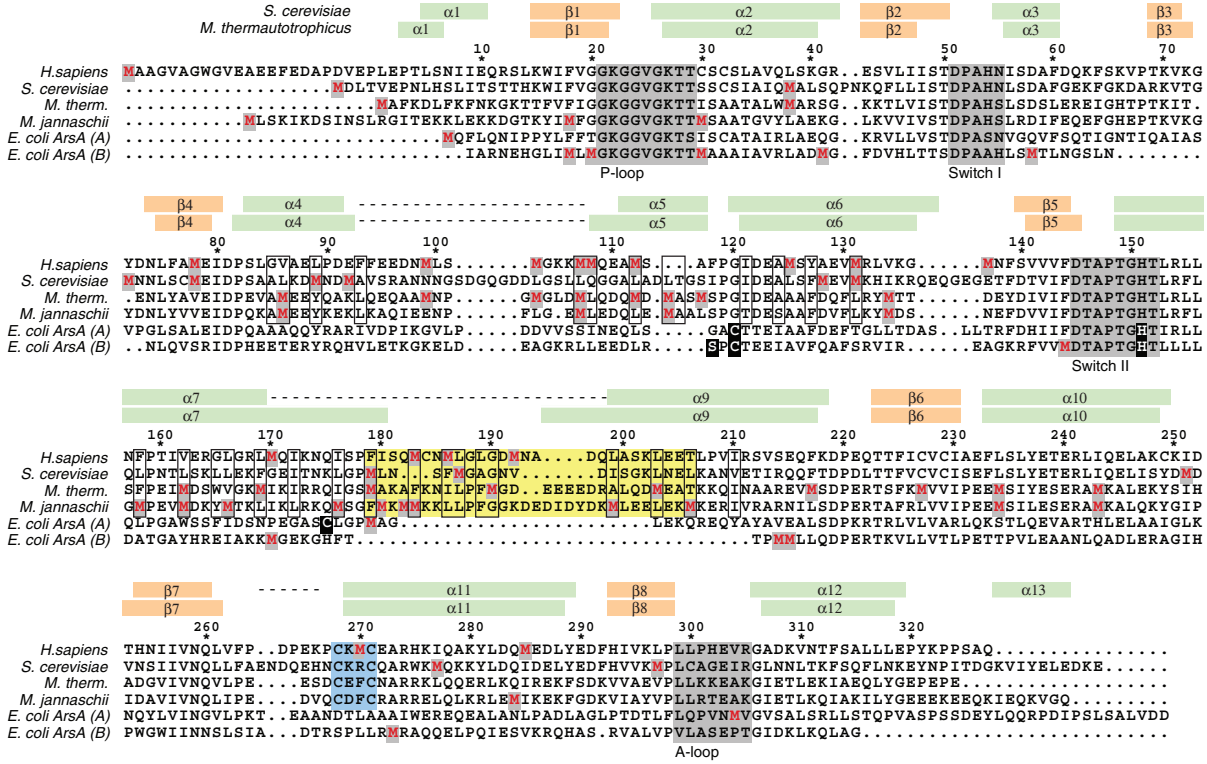

Figure 2: Sequence alignment of eukaryotic and archaeal TRC40/Get3 orthologs with the functionally distinct bacterial ArsA. Numbering is according to *M. thermautotrophicus* TRC40. Secondary structure elements (green, orange) and disordered regions (dashed lines) are indicated for MtTRC40 and ScGet3. The four conserved ATPase sequence motifs are highlighted in gray. The 'TRC40-insert' (yellow) and the zinc-binding 'CXXC motif' (blue) are indicated. Hydrophobic residues lining the MtTRC40 composite groove are boxed. Methionine residues are in red; *E. coli* ArsA residues involved in antimony binding are in white.

archaeal genomes. Thus, whether a membrane receptor for MtTRC40 exists or is required for efficient insertion remains to be determined.

Alternatively, the single membrane architecture of archaea may obviate the need for a dedicated TRC40 receptor, with TA protein insertion occurring instead by an 'unassisted' mechanism (18) facilitated by the lipid composition of the archaeal plasma membrane. In this view, TRC40 is serving solely as a chaperone, with its targeting function coevolving with diversification of intracellular membranes. Defining the mechanistic basis of TA protein capture and insertion in this minimal archaeal system is an important goal for future studies.

Methods

Protein cloning, expression and purification

The gene encoding full-length *M. thermautotrophicus* TRC40 was amplified by polymerase chain reaction (PCR) from genomic DNA and subcloned into pCDF-1b (Novagen). This construct was cotransformed with C-terminally 6xHis-tagged *Methanococcus jannaschii* Sec61β in pET21c (Novagen) into *Escherichia coli* BL21(DE3)/pRIL (Novagen). Expression was carried out at room temperature for ~12 h by induction with 0.1 mM isopropyl β-D-1-thiogalactopyranoside (IPTG) after the cells reached an A_{600} of ~0.6. Cells were disrupted in lysis buffer [50 mM Tris, pH 7.5, 500 mM NaCl, 5 mM β-mercaptoethanol, 10 mM imidazole, 5% glycerol, 20 μg/mL Dnase1 and 1 mM phenylmethylsulphonyl fluoride (PMSF)] using a high-pressure microfluidizer (Avestin). After clearing by centrifugation, the supernatant was batch-purified by nickel affinity chromatography (Ni-NTA His Bind Resin; Novagen) followed by gel filtration (Superdex 200 10/300 GL; GE Healthcare). Uncomplexed MtTRC40 dimer fractions were pooled, repurified by gel filtration, concentrated to ~5–10 mg/mL in 10 mM Tris, pH 7.5, 150 mM NaCl and 2 mM DTT, and stored at −80°C. For biochemical analysis, the gene encoding MtTRC40 was subcloned into a pET28 derivative (Novagen) modified to incorporate a tobacco etch virus (TEV) protease cleavage site between an N-terminal 6xHis tag and the polylinker; 6xHis-tagged protein was purified by nickel affinity and size-exclusion chromatography essentially as described above.

Crystallization, data collection and refinement

Crystals of MtTRC40 complexed with ADP•AlF_4^- were grown at room temperature using hanging drop vapor diffusion by mixing equal volumes of an ~6 mg/mL protein solution containing 2 mM ADP, 2 mM $MgCl_2$, 2 mM $AlCl_3$ and 8 mM NaF with a reservoir solution containing 34% pentaerythritol propoxylate (5/4 PO/OH), 50 mM HEPES, pH 7.0 and 25 mM KCl. Crystals were flash frozen directly in liquid nitrogen. Data were collected at APS beamline 21-IDF ($\lambda = 0.97856$) and processed using HKL2000 (HKL Research).

The structure was determined by molecular replacement with PHASER (19) using the closed-dimer form of *S. cerevisiae* Get3 (2WOJ) with the α-helical subdomain removed as the search model. A data set to 2.1 Å was used for model building and refinement with COOT (20) and PHENIX (21). The final model contains two MtTRC40 homodimers, four Mg^{2+}ADP•AlF_4^-

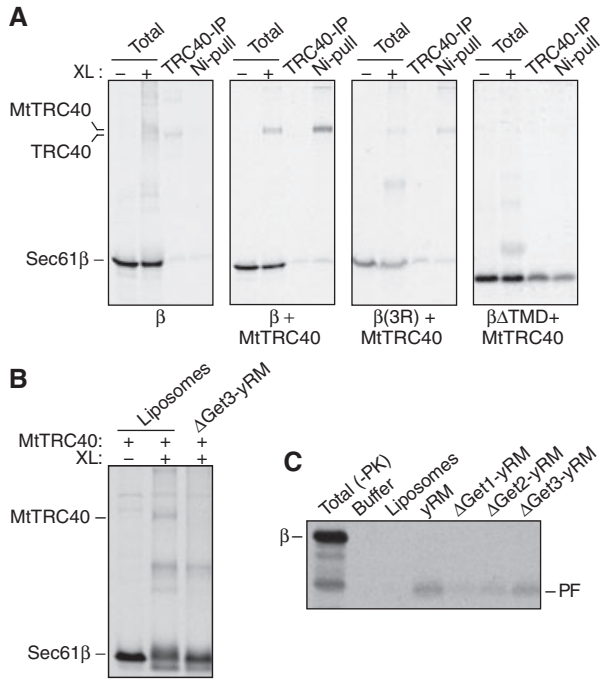

Figure 3: TA substrate binding and insertion by MtTRC40. A) Full-length human Sec61β, an insertion-deficient triple arginine mutant (3R) or a construct lacking its TMD (ΔTMD), was synthesized in RRL in the presence or absence of 100 ng/μL recombinant 6xHis-tagged MtTRC40. Fractions from a sucrose gradient were treated with an amine-specific cross-linker and pulled-down using anti-TRC40 antibodies ('TRC40-IP') or Ni-NTA sepharose beads ('Ni-pull'). The positions of non-cross-linked Sec61β and the major cross-linked partner (endogenous mammalian TRC40 or recombinant MtTRC40) are indicated. B) Sec61β was synthesized in PD-RRL supplemented with 5 ng/μL MtTRC40, incubated with liposomes or yeast rough microsomes prepared from a ΔGet3 strain (ΔGet3-yRM) and then subjected to chemical cross-linking. C) Sec61β was synthesized in PD-RRL supplemented with 5 ng/μL MtTRC40. After incubation with the indicated vesicles, insertion was monitored using a protease protection assay described previously (7,18). The PF diagnostic of proper insertion of the TA substrate is indicated.

complexes, two zinc atoms and 433 water molecules, and was refined to an *R*-factor (R_{free}) of 17.7% (22.5%). No electron density was observed for residues: 1, 94-114 and 323-324 in chain A; 1, 93-105, 179-198 and 323-324 in chain B; 1, 92-115, 180-191 and 322-324 in chain C and 1, 94-106 and 322-324 in chain D.

Cross-linking assay

Full-length ^{35}S-labeled human Sec61β or its mutants were synthesized in an RRL translation extract in the presence or absence of 100 ng/μL 6xHis-tagged MtTRC40. After translation for 30 min at 32°C, the mixture was subjected to 5–25% (w/v) sucrose gradient in physiological salt buffer (50 mM HEPES, pH 7.4, 100 mM potassium acetate, 7 mM magnesium acetate) for 5 h at 259 000 × ***g*** at 4°C. Ten fractions were collected manually from the sucrose gradient. Fractions 4–6 were pooled and Disuccinimidyl suberate (DSS) cross-linker was added to a final concentration of 250 μM. After incubating for 30 min at room temperature, the reaction was terminated by adding 100-fold molar excess of Tris–HCl, pH 7.5. Samples were boiled with 1% SDS and diluted with 10-fold excess of immunoprecipitation buffer (IP: 50 mM Tris, pH 7.5, 150 mM NaCl, 1% Triton-X-100) at 4°C. Anti-TRC40 antibodies (against human TRC40) or Ni-NTA Sepharose beads were added and incubated with mixing for 90 min at 4°C. To recover the immunoglobulins, protein A agarose beads were added and mixed for 90 min at 4°C. The beads were washed 3× with 1 mL of IP buffer, eluted with SDS–PAGE sample buffer and analyzed by 12% Tris–Tricine gel and autoradiography. Cross-linking was also performed in the absence of endogenous mammalian TRC40 using a phenyl- and Diethylaminoethyl (DEAE)-Sepharose-depleted RRL (PD-RRL) translation extract (see below). Following synthesis of Sec61β in the presence or absence of 5 ng/μL 6xHis-tagged MtTRC40, ribosomes were removed by centrifugation and cross-linking was carried out on the supernatant as described above.

Insertion assay

Full-length ^{35}S-labeled human Sec61β containing a double strep-tag at the N-terminus and a 3F4 epitope tag at the C-terminus was synthesized in PD-RRL supplemented with 5 ng/μL of 6xHis-tagged MtTRC40. After removing ribosomes by centrifugation, the supernatant was tested for insertion into liposomes or yRMs (prepared from wild-type or Get-deletion strains from Open Biosystems) in the presence of an energy-regenerating system (2 mM ATP, 10 mM creatine phosphate and 40 μg/mL creatine kinase). After incubating at 32°C for 30 min, the samples were treated with proteinase K (0.5 mg/mL) for 60 min on ice. The protease protected fragment (PF) was immunoprecipitated with an antibody against the 3F4 tag at the C-terminus of Sec61β.

Miscellaneous

Liposomes containing egg phosphatidylcholine and dipalmotyl phosphatidylethanolamine in a 4:1 (w/w) ratio were prepared by extrusion through 100-nm polycarbonate filter. Depleted RRL translation extract was prepared by removing ribosomes by centrifugation and passing the supernatant over a phenyl-Sepharose column. The flow-through was bound to and eluted from a DEAE-Sepharose column, and the depleted translation extract (PD-RRL) was reconstituted from the DEAE elution and ribosomes. This lysate is devoid of TRC pathway chaperones, and is deficient for TA substrate insertion unless supplemented with physiological concentrations of TRC40/Get3 (Figure S2).

Acknowledgments

Data were collected at beamline 21-IDF at the Advanced Photon Source (APS), Argonne National Laboratory, and we thank the beamline staff for support. Use of the Advanced Photon Source, an Office of Science User Facility operated for the US Department of Energy (DOE) Office of Science by Argonne National Laboratory, was supported by the US DOE under Contract No. DE-AC02-06CH11357. We thank Maureen Downing for cloning the *M. thermautotrophicus* TRC40 homolog, and Agnieszka Mateja and Malgorzata Dobosz for help with data collection. This work was supported by the Intramural Research Program of the NIH (to RSH), NIH grant T32 GM008720 (to JS), an Edward Mallinckrodt, Jr Foundation Grant (to RJK) and NIH Grant R01 GM086487 (to RJK). JS and PD carried out cloning, protein purification and crystallization. JS, PD and RJK performed data collection and JS carried out the structure determination and model building. MM and RSH performed the substrate-binding and membrane insertion assays. RJK conceived the project, guided experiments and wrote the article. All authors discussed the results and commented on the manuscript. The X-ray structure of Mg^{2+}ADP•AlF_4^--bound *M. thermautotrophicus* TRC40 is deposited in the Protein Data Bank under ID code 3zq6.

Supporting Information

Additional Supporting Information may be found in the online version of this article:

Table S1: Data collection and refinement statistics.

Figure S1: Cross-eyed stereo view of electron density for the Mg^{2+} ADP•AlF_4^- complex of *M. thermautotrophicus* TRC40. The refined model is superimposed onto a σ_A-weighted $2F_o - F_c$ map calculated at 2.1 Å resolution and contoured at 2σ.

Figure S2: Characterization of the depleted translation extract (PD-RRL). Sec61β was translated in PD-RRL in the presence or absence of recombinant yeast Get3. An aliquot was subjected to chemical cross-linking with DSS to evaluate substrate interactions with 5 ng/μL Get3 (top panel). The remainder was incubated with yRMs and analyzed for insertion by the protease protection assay (bottom panel). PD-RRL lacks all known chaperones that interact with ER-directed TA proteins, and is deficient for insertion; activity was restored by supplementing with physiological levels of TRC40/Get3.

Please note: Wiley-Blackwell are not responsible for the content or functionality of any supporting materials supplied by the authors. Any queries (other than missing material) should be directed to the corresponding author for the article.

References

1. Kutay U, Hartmann E, Rapoport TA. A class of membrane proteins with a C-terminal anchor. Trends Cell Biol 1993;3:72–75.
2. Beilharz T, Egan B, Silver PA, Hofmann K, Lithgow T. Bipartite signals mediate subcellular targeting of tail-anchored membrane proteins in *Saccharomyces cerevisiae*. J Biol Chem 2003;278:8219–8223.
3. Kalbfleisch T, Cambon A, Wattenberg BW. A bioinformatics approach to identifying tail-anchored proteins in the human genome. Traffic 2007;8:1687–1694.
4. Kriechbaumer V, Shaw R, Mukherjee J, Bowsher CG, Harrison AM, Abell BM. Subcellular distribution of tail-anchored proteins in Arabidopsis. Traffic 2009;10:1753–1764.
5. Favaloro V, Spasic M, Schwappach B, Dobberstein B. Distinct targeting pathways for the membrane insertion of tail-anchored (TA) proteins. J Cell Sci 2008;121:1832–1840.
6. Favaloro V, Vilardi F, Schlecht R, Mayer MP, Dobberstein B. Asna1/TRC40-mediated membrane insertion of tail-anchored proteins. J Cell Sci 2010;123:1522–1530.
7. Stefanovic S, Hegde RS. Identification of a targeting factor for posttranslational membrane protein insertion into the ER. Cell 2007;128:1147–1159.
8. Schuldiner M, Metz J, Schmid V, Denic V, Rakwalska M, Schmitt HD, Schwappach B, Weissman JS. The GET complex mediates insertion of tail-anchored proteins into the ER membrane. Cell 2008;134:634–645.
9. Borgese N, Fasana E. Targeting pathways of C-tail-anchored proteins. Biochim Biophys Acta 2011;1808:937–946.
10. Leznicki P, Clancy A, Schwappach B, High S. Bat3 promotes the membrane integration of tail-anchored proteins. J Cell Sci 2010;123:2170–2178.
11. Mariappan M, Li X, Stefanovic S, Sharma A, Mateja A, Keenan RJ, Hegde RS. A ribosome-associating factor chaperones tail-anchored membrane proteins. Nature 2010;466:1120–1124.
12. Wang F, Brown EC, Mak G, Zhuang J, Denic V. A chaperone cascade sorts proteins for posttranslational membrane insertion into the endoplasmic reticulum. Mol Cell 2010;40:159–171.
13. Chang Y-W, Chuang Y-C, Ho Y-C, Cheng M-Y, Sun Y-J, Hsiao C-D, Wang C. Crystal structure of Get4-Get5 complex and its interactions with Sgt2, Get3, and Ydj1. J Biol Chem 2010;285:9962–9970.
14. Vilardi F, Lorenz H, Dobberstein B. WRB is the receptor for TRC40/Asna1-mediated insertion of tail-anchored proteins into the ER membrane. J Cell Sci 2011;124:1301–1307.
15. Jonikas MC, Collins SR, Denic V, Oh E, Quan EM, Schmid V, Weibezahn J, Schwappach B, Walter P, Weissman JS, Schuldiner M. Comprehensive characterization of genes required for protein folding in the endoplasmic reticulum. Science 2009;323:1693–1697.
16. Copic A, Dorrington M, Pagant S, Barry J, Lee MC, Singh I, Hartman JL IV, Miller EA. Genomewide analysis reveals novel pathways affecting endoplasmic reticulum homeostasis, protein modification and quality control. Genetics 2009;182:757–769.
17. Borgese N, Righi M. Remote origins of tail-anchored proteins. Traffic 2010;11:877–885.
18. Brambillasca S, Yabal M, Soffientini P, Stefanovic S, Makarow M, Hegde RS, Borgese N. Transmembrane topogenesis of a tail-anchored protein is modulated by membrane lipid composition. EMBO J 2005;24:2533–2542.
19. Mateja A, Szlachcic A, Downing ME, Dobosz M, Mariappan M, Hegde RS, Keenan RJ. The structural basis of tail-anchored membrane protein recognition by Get3. Nature 2009;461:361–366.
20. Bozkurt G, Stjepanovic G, Vilardi F, Amlacher S, Wild K, Bange G, Favaloro V, Rippe K, Hurt E, Dobberstein B, Sinning I. Structural insights into tail-anchored protein binding and membrane insertion by Get3. Proc Natl Acad Sci U S A 2009;106:21131–21136.
21. Hu J, Li J, Qian X, Denic V, Sha B. The crystal structures of yeast Get3 suggest a mechanism for tail-anchored protein membrane insertion. PLoS ONE 2009;4:e8061.
22. Suloway CJ, Chartron JW, Zaslaver M, Clemons WM Jr. Model for eukaryotic tail-anchored protein binding based on the structure of Get3. Proc Natl Acad Sci U S A 2009;106:14849–14854.
23. Yamagata A, Mimura H, Sato Y, Yamashita M, Yoshikawa A, Fukai S. Structural insight into the membrane insertion of tail-anchored proteins by Get3. Genes Cells 2010;15:29–41.